

# Design, Synthesis and Studies of Novel Imidazoles <sup>†</sup>

Priyanka Chandra\*, Swastika Ganguly <sup>1</sup> and Manik Ghosh<sup>2\*</sup>

<sup>1</sup> Professor, Department of Pharmaceutical Technology and Sciences, Birla Institute of Technology, Mesra, Ranchi, India ; swastikagangu-ly@bitmesra.ac.in

<sup>2</sup> Associate Professor, Department of Pharmaceutical Technology and Sciences, Birla Institute of Technology, Mesra, Ranchi, India ; man-ik@bitmesra.ac.in

\* Correspondence: priyankachandra78@gmail.com, manik@bitmesra.ac.in ;

<sup>†</sup> Presented at the 25th International Electronic Conference on Synthetic Organic Chemistry, 15-30 November 2021; Available online: <https://ecsoc-25.sciforum.net/>.

**Abstract:** Twenty five novel imidazole analogs **26(a-r)** & **27(a-g)** were designed, based on QSAR studies. The designed compounds were subjected to molecular docking studies and predictive ADME studies were performed. Molecular docking studies were performed in the active site of HIV-1-reverse transcriptase PDB ID: 1RT2 & glucosamine-fructose-6-phosphate animotransferase PDB ID: 2VF5. AutoDock tools v1.5.6 was used for the molecular docking studies. The binding mode analysis of the compounds was done. Docking studies suggested that all the compounds showed good interactions i.e., H-bonding interactions and pi-pi interactions when compared to the standard compounds i.e., nevirapine (in case of PDB ID:1RT2) and metronidazole (in case of PDB ID:2VF5). The predictive ADME studies also showed that all the compounds have drug-like properties. The results show that these compounds can be synthesised and further explored for their possible anti-microbial and antiviral activities.

**Keywords:** imidazole; QSAR; molecular docking; binding mode analysis; ADME

**Citation:** Ghosh, M.; Ganguly, S.; Chandra, P. Design, Synthesis and Studies of Novel Imidazoles. *Chem. Proc.* **2021**, *3*, x. <https://doi.org/10.3390/xxxxx>

Academic Editor: Julio A. Seijas

Published: 15 November 2021

**Publisher's Note:** MDPI stays neutral with regard to jurisdictional claims in published maps and institutional affiliations.



**Copyright:** © 2021 by the authors. Submitted for possible open access publication under the terms and conditions of the Creative Commons Attribution (CC BY) license (<https://creativecommons.org/licenses/by/4.0/>).

## 1. Introduction

Compounds containing the imidazole (1) nucleus exhibit various activities viz. anti-protozoal [1–3], antibacterial, antifungal, antiviral and other various activities [1].

The various drugs that are used in the clinical practice as effective antiprotozoal, antiviral, antibacterial, antifungal agents containing the imidazole nucleus are azomycin (2), metronidazole (3), secnidazole (4), ornidazole(5), benznidazole (6), tinidazole (7), nimorazole (8), megazol (9), dimetridazole (10), carnidazole (11), panidazole (12), misonidazole (13), Clotrimazole (14), Isoconazole (15), Miconazole (16), Econazole (17), butoconazole (18), oxiconazole (19), Climbazole (20), Ketoconazole (21), Sertaconazole (22), Flutrimazole (23), Eberconazole (24) and luliconazole (25) [1,4–18].

Human Immuno Deficiency Virus is a single stranded RNA virus that belongs to retroviridae family. It leads to development of a deadly disease called AIDS [19]. The enzyme reverse transcriptase helps in the reverse transcription of cDNA, and plays a crucial role in the the life cycle of the virus. HIV infections are blocked by targeting various steps of the life cycle of the virus like- the cell attachment of the virus to human, virus entry to cell, uncoating of virus etc. Various enzymes like reverse transcriptase, protease, integrase plays a vital role in different processes of the viral life cycle and various classes of drugs helps inhibiting these enzymes like Non-Nucleoside reverse transcriptase inhibitors (NNRTIs), Nucleoside reverse transcriptase inhibitors (NRTIs), Protease inhibitors, Nucleotide reverse transcriptase inhibitors (NtRTIs) etc. HIV is sub- categorized into two types: HIV-1 & HIV-2, causing infections worldwide and the infections confined to west part of Africa only respectively. The mechanism of action of the various classes of drugs are different thus acting in different phases of HIV infection and subsequently inhibiting

the entry and growth of the virus within the host body [20–22]. Imidazole derivatives has been found to exhibit antibacterial effects as well.<sup>1</sup> The antibacterial effects of 1-alkyl imidazole derivatives increase as the number of carbon in alkyl chain increases upto 9 carbons. Also substitution of methyl and nitro groups at 2 and 4-positions respectively on imidazole ring increases the antibacterial activity of the scaffold [23]. Antibacterial activity can be targeted through various pathways, one such is- through inhibition of hexosamine metabolism pathway [24]. The blocking of this pathway is utilised in this current study, for the checking the antibacterial effects of the designed compounds.

## 2. Materials & Methods

Autodock v 4.5.6, was used for carrying out the computational studies [25], installed in a HP Precision workstation (Radeon Graphics) with an Intel Core 3 quad processor and 8 GB of RAM with Operating system as Windows 10.

- **Docking Strategies:**

The binding of drugs in various binding sites can be predicted by using molecular docking studies. For structure-based drug designing of drugs in pharmaceutical sciences, it is a very commonly used method. The different conformations by which it binds to the target site can be easily analyzed by this method. Binding affinity has an important role in the rational drug designing.

In the present study we have used two receptors, viz. HIV-1-reverse transcriptase, PDB ID: 1RT2 & Glucosamine-fructose-6-phosphate animotransferase PDB ID: 2VF5. The internal ligand present in the receptors are TNK (29) and GLP(28) respectively. The standard drugs that are used for docking the receptors are Nevirapine(30) and Metronidazole(3) respectively.

In HIV-1-reverse transcriptase PDB ID: 1RT2, the Non-nucleoside Inhibitory Binding Pocket (NNIBP) is formed due to the changes in the conformation of 3D structure of reverse transcriptase, which is induced by the non-competitive binding of NNRTIs. Various amino acid residues that are present in NNIBP play a major role in the interaction with NNRTIs [26].

In Glucosamine-fructose-6-phosphate animotransferase PDB ID: 2VF5, the catalytic activation occurs due to glutamine binding after D-fructose 6-phosphate binds to the catalytic site and thereby release of D-glucosamine 6-phosphate as the end product of the 1<sup>st</sup> step of hexosamine metabolism [24].

The molecular modelling studies were carried on two sets of designed novel imidazole analogs **26(a-r)** & **27(a-g)** respectively.

- **Molecular Modelling Studies:**

- i. **Protein Preparation:**

The X-ray-co-crystallized structures of all of the protein molecules (PDB ID: 1RT2, 2VF5) used in the study were retrieved from the Research Collaboratory for Structural Bioinformatics (RCSB) [27]. From every protein molecule co-crystallized water molecule were deleted and polar hydrogens were added as well as Gasteiger charges were assigned and it was saved in PDBQT format using AutoDock 4.2.6 software.

- ii. **Ligand Preparation:**

All of the ligands were prepared by minimizing their energies using PRODRG server [28]. PDBQT format of all of the ligands were saved.

- iii. **Receptor grid Generation:**

Autogrid was used to generate specific grid maps for each and every ligand. The generation of the grid box was done by taking the dimensions of the three coordinates (X, Y and Z) at 24 × 24 × 24, with grid spacing of 0.100 Å. The values of X, Y and Z centre's were taken according to the crystallographic positions of the native ligand of each receptor.



#### iv. Docking Protocol Validation:

For computational studies, AutoDock 4.2.6 was used. This software was used to predict the different binding mode of co-crystallized ligands as well as test molecules with all of the receptors taken to carry out the study.

To carry out the docking procedure the method was validated to check the robustness of the software. The extracted ligand (previously mentioned) was corrected and then it was redocked using the same protein. The standard drugs were docked into the active site of the respective receptors along with the other test molecules using the same procedure and thereafter the different conformations were compared. The generated docking scores and conformations of the co-crystallized ligand and the standard drugs were compared with the docking scores of other test molecules to choose the best molecule. The results are mentioned in Table 3.

### 3. Predictive ADME Studies

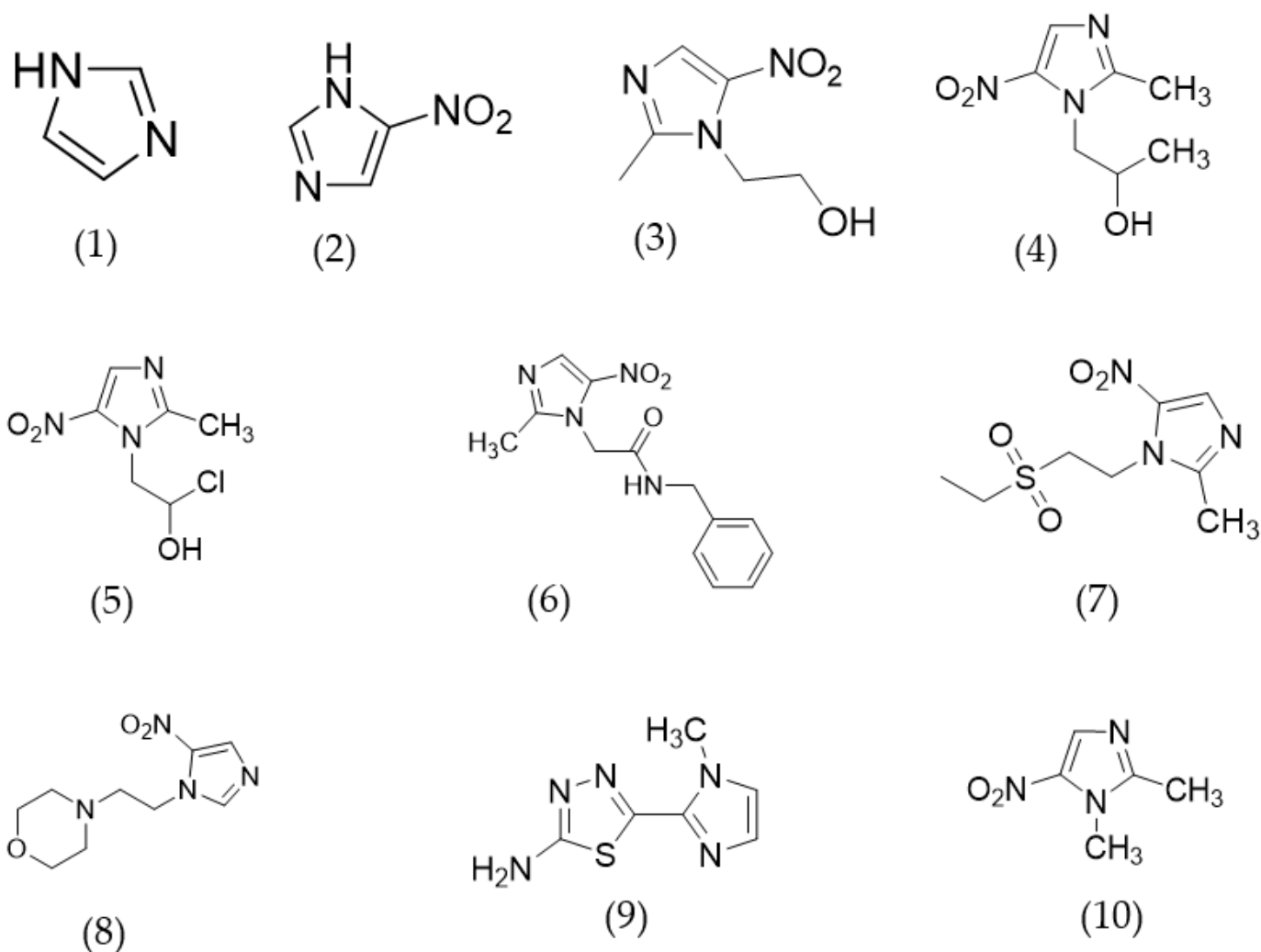
The predictive ADME studies were done by using SwissADME [29], which is a free web tool provided by Swiss Institute of Bioinformatics, using Google chrome web browser installed in a single machine running on a 2.30 GHz Intel Core i5 processor with WINDOWS-8 as the Operating System. The analysis of Physicochemically important descriptors and Pharmacokinetically relevant properties of the ligands can be performed and well predicted by using this online tool. The most important descriptors are reported in the Table 4, which are required for predicting the drug-like properties of the ligands.

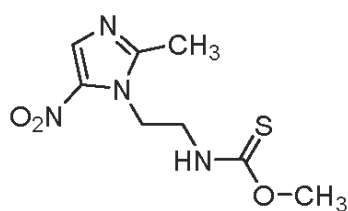
The test compounds were built on the server website (<http://www.swissadme.ch>) by using the molecule sketcher (based on Chem Axon's Marvin JS—<http://www.chemaxon.com>) available on the webpage [29]. This structure was converted to SMILES list (the actual input for the programme to run) and then clicked on Run in order to run the calculations which gets activated when the list is not empty. The physicochemical properties, lipophilicity, drug likeliness, etc were observed which was essential to ensure drug like pharmacokintetic profile while using rational drug design.

### 4. Results and Discussions

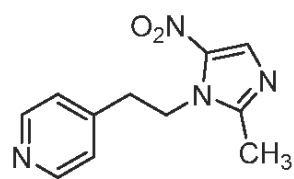
In this work we have considered the crystal structures of HIV-1-reverse transcriptase (PDB Id-1RT2) and the crystal structure of glucosamine-fructose-6-phosphate aminotransferase (PDB Id-2VF5), Co-crystallised with the ligands TNK 651 (29) and GLP (28) respectively. Docking studies were done using AutoDock Tools (V-4.5.6), on the selected crystal structures. The designed compounds were studied in the Non-nucleoside inhibitory binding pocket of the HIV-1 reverse transcriptase receptor. The docking scores and the binding poses of the different NNRTI's were studied, the results are given in Table 3. The software used for docking purpose was validated at first, to check its reliability for further docking procedures. The internal ligands were removed from the receptors and were redocked into the active site of the protein. Root mean square deviation (RMSD) values of 0.0 Å were obtained for the internal ligands-TNK 651(29) & GLP(28) for the HIV-1 reverse transcriptase and glucosamine-fructose-6-phosphate aminotransferase with PDB Id-1RT2 & 2VF5 respectively. As the RMSD values were within the standard limits (i.e, 0.2 Å), the software was used for further docking procedures. In the receptor (PDB Id-2VF5), the docking score of the internal ligand was found to be -7.9, in the same active site, the docking score of the standard drug- metronidazole was found to be -7.5. Amongst the designed compounds, the best interaction was shown by two compounds- **26n** and **26o**, with a dock score of -6.7 and -7.4 respectively, in the binding pocket of 2VF5. The binding mode analysis, revealed that the compound **26n** had 6-hydrogen bond interactions with six amino acids of the binding pocket-ALA602, GLN348, GLU488, VAL399, SER303 and SER401 with a bond length of 2.1 Å, 2.2 Å, 2.4 Å, 2.5 Å, 2.6 Å & 2.9 Å, i.e., 26n O-phenyl ring---NH ALA602 = 2.1Å, 26n N-Imidazole ring---NH GLN348 = 2.2Å, 26n NH-phenyl ring---O GLU488 = 2.4Å, 26n OH-propyl chain---O VAL399 = 2.5Å, 26n N-Imidazole ring---OH SER303 = 2.6Å, 26n OH-propyl chain---O

SER401 = 2.9 Å, whereas the compound **26o** had 8-hydrogen bonding interactions with three amino acids of the binding pocket- SER303, THR 302 and SER401 with a bond length of 2.1, 2.2, 1.9, 2.0, 2.9, 3.1,3.3 & 3.3 Å, i.e.,  $26o_{O-NO_2} \cdots NH_{SER303} = 2.1 \text{ \AA}$ ,  $26o_{O-NO_2} \cdots NH_{THR302} = 2.2 \text{ \AA}$ ,  $26o_{NH} \cdots OSER401 = 1.9 \text{ \AA}$ ,  $26o_{NH} \cdots OSER401 = 2.0 \text{ \AA}$ ,  $26o_{NH} \cdots OH_{SER401} = 2.9 \text{ \AA}$ ,  $26o_{OH} \cdots OSER401 = 3.1 \text{ \AA}$ ,  $26o_{OH} \cdots NH_{SER401} = 3.3 \text{ \AA}$ ,  $26o_{NH} \cdots OSER401 = 3.3 \text{ \AA}$  (Figures 1 and 2). In the receptor (PDB Id-1RT2), the docking score of the internal ligand was found to be -11.9, in the same active site, the docking score of the standard drug- nevirapine was found to be -9.5. Amongst the designed compounds, the best interaction was shown by two compounds- **26p** and **26q**, with a dock score of -8.2 and -8.3 respectively, in the binding pocket of 1RT2. The binding mode analysis, revealed that the compound **2p** had 4-hydrogen bond interactions with three amino acids of the binding pocket- LYS101, LYS103 and VAL106 with a bond length of 2.3 Å, 2.3 Å, 2.6 Å & 2.2 Å, i.e.,  $26p_{OH-propyl\ chain} \cdots O_{LYS101} = 2.3 \text{ \AA}$ ,  $26p_{NH-phenyl\ ring} \cdots O_{LYS103} = 2.3 \text{ \AA}$ ,  $2p_{OH-propyl\ chain} \cdots NH_{LYS103} = 2.6 \text{ \AA}$ ,  $26p_{NO-phenyl\ ring} \cdots NH_{VAL106} = 2.2 \text{ \AA}$ , similarly, the compound **26q** had 3- hydrogen bond interactions with three amino acids of the binding pocket-VAL106, LYS103 and TYR316 with a bond length of -2.0 Å, 2.7 Å, & 2.8 Å, i.e.,  $26q_{NO-Benzene} \cdots NH_{VAL106} = 2.0 \text{ \AA}$ ,  $26q_{OH-phenyl\ ring} \cdots NH_{LYS103} = 2.7 \text{ \AA}$ ,  $26q_{NH-phenyl\ ring} \cdots OH_{TYR316} = 2.8 \text{ \AA}$  (Figures 3 and 4).

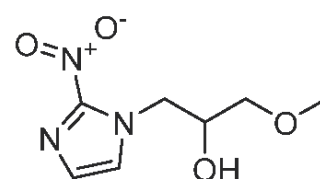




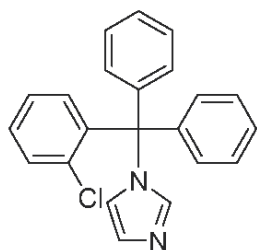
(11)



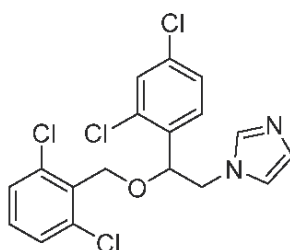
(12)



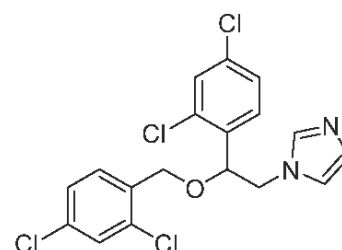
(13)



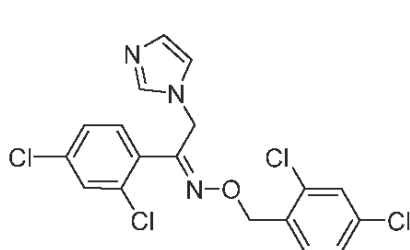
(14)



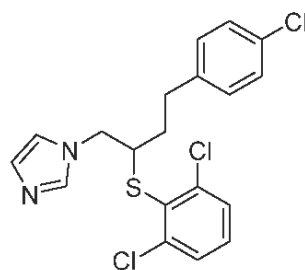
(15)



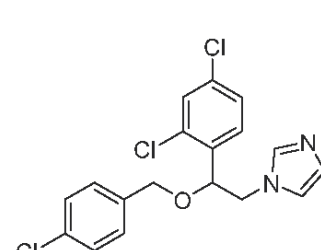
(16)



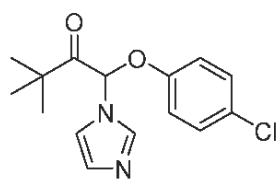
(17)



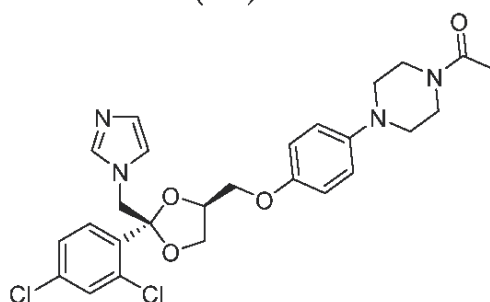
(18)



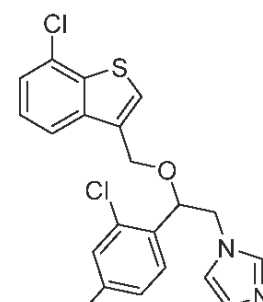
(19)



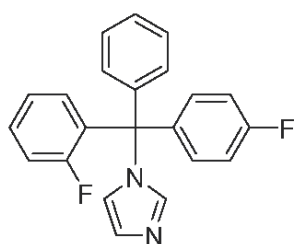
(20)



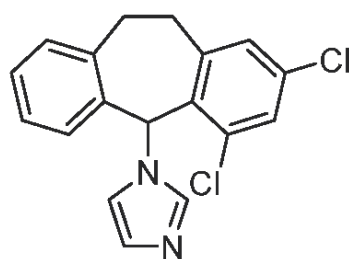
(21)



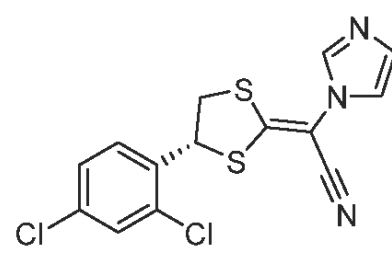
(22)



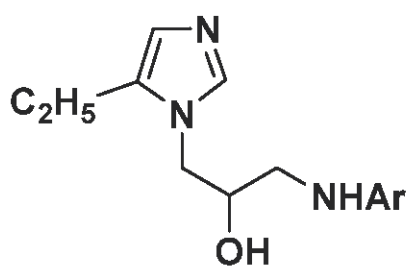
(23)



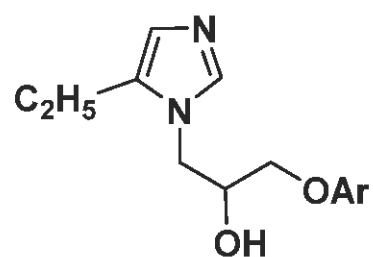
(24)



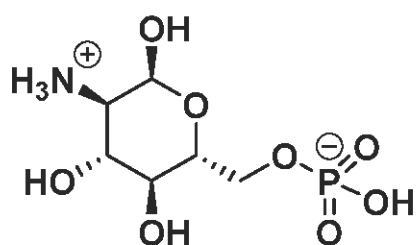
(25)



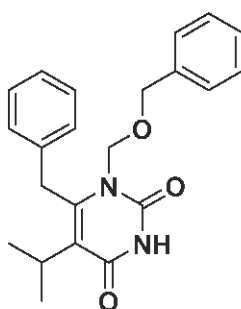
26(a-r)



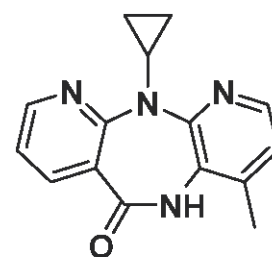
27(a-g)



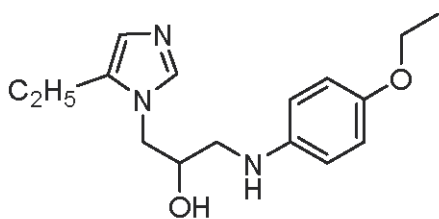
(28)



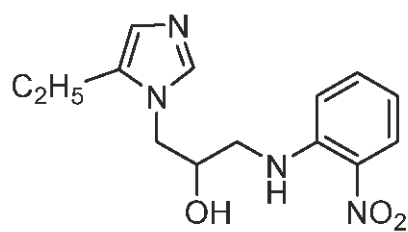
(29)



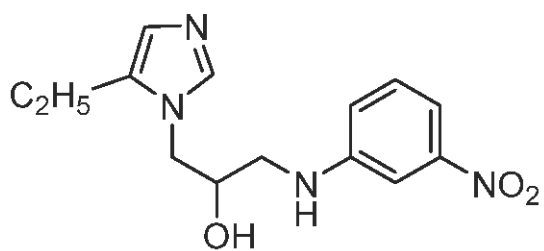
(30)



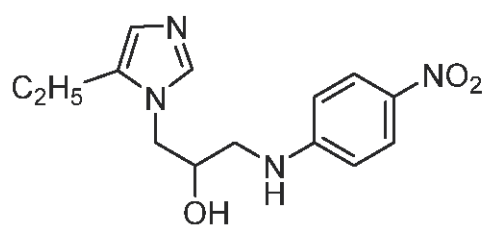
(26n)



(26o)

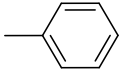
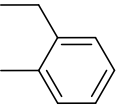
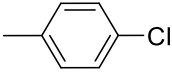
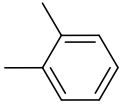
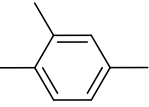
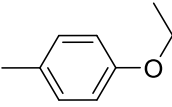
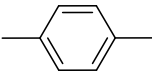
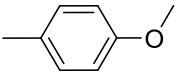
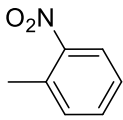
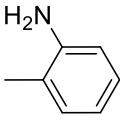
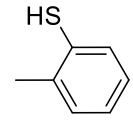
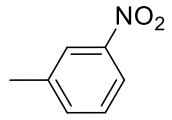
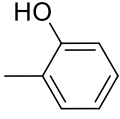
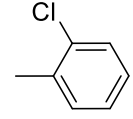
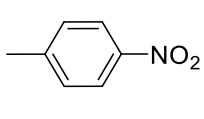
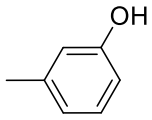
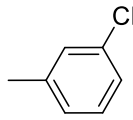
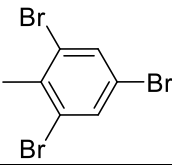


(26p)

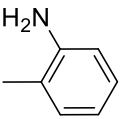
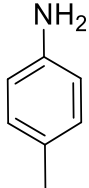
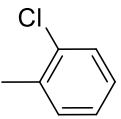
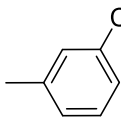
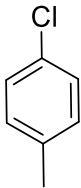
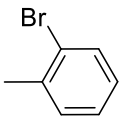
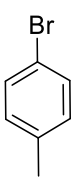


(26q)

**Table 1.** List of substituted anilines in 26(a-r).

Compound	Ar	Compound	Ar	Compound	Ar
26a		26g		26m	
26b		26h		26n	
26c		26i		26o	
26d		26j		26p	
26e		26k		26q	
26f		26l		26r	

**Table 2.** List of substituted phenols in 27(a-g).

Compound	27a	27b	27c	27d	27e	27f	27g
Ar							

**Table 3.** Docking scores of the designed compounds in active site of HIV-1-reverse transcriptase PDB ID: 1RT2 and glucosamine-fructose-6-phosphate aminotransferase PDB ID: 2VF5.

Compound	Docking Scores on	
	1RT2	2VF5
Native Ligand	-11.9	-7.9
Standard Drug	-9.5	-7.5
26a	-8.3	-6.3
26b	-8.6	-6.2
26c	-8.3	-6.4
26d	-7.9	-6.8
26e	-7.9	-6.8
26f	-7.9	-6.6
26g	-8.6	-6.6
26h	-8.4	-6.4
26i	-7.8	-6.1



<b>26j</b>	-7.9	-6.1
<b>26k</b>	-8.3	-6.3
<b>26l</b>	-8.6	-6.7
<b>26m</b>	-7.9	-6.7
<b>26n</b>	-7.9	-6.7
<b>26o</b>	-8.1	-7.4
<b>26p</b>	-8.2	-7.1
<b>26q</b>	-8.3	-7.4
<b>26r</b>	-5.2	-6.6
<b>27a</b>	-8.3	-7.2
<b>27b</b>	-8.2	-7.2
<b>27c</b>	-8.7	-7.0
<b>27d</b>	-8.7	-7.4
<b>27e</b>	-8.1	-7.1
<b>27f</b>	-8.3	-7.0
<b>27g</b>	-8.0	-7.0

**Table 4.** Predictive ADME studies of the designed compounds.

Compound	Mol. Wt.	HBA	HBD	MR	TPSA	Log P <sub>o/w</sub>	Solubility (mg/mL)	Lipinski	Veber's	Leadlikeness
<b>26a</b>	245.32	4	2	72.28	35.5	1.30	1.30	Yes	Yes	No
<b>26b</b>	259.35	4	2	77.63	35.5	1.56	1.55	Yes	Yes	Yes
<b>26c</b>	259.35	4	2	77.63	35.5	1.56	2.01	Yes	Yes	Yes
<b>26d</b>	260.33	5	3	75.02	61.52	0.47	2.24	Yes	Yes	Yes
<b>26e</b>	261.32	5	5	73.48	55.73	0.47	1.52	Yes	Yes	Yes
<b>26f</b>	261.32	5	3	73.48	55.73	0.47	1.52	Yes	Yes	Yes
<b>26g</b>	273.37	4	2	82.44	35.5	1.81	9.23	Yes	Yes	Yes
<b>26h</b>	273.37	4	2	82.99	35.5	1.81	9.17	Yes	Yes	Yes
<b>26i</b>	275.35	5	2	78.21	44.73	0.73	7.09	Yes	Yes	Yes
<b>26j</b>	277.39	4	2	80.24	74.3	1.3	3.15	Yes	Yes	Yes
<b>26k</b>	279.77	4	2	77.11	35.5	1.56	1.99	Yes	Yes	Yes
<b>26l</b>	279.77	4	2	77.11	35.5	1.56	1.99	Yes	Yes	Yes
<b>26m</b>	279.77	4	2	77.11	35.5	1.56	1.99	Yes	Yes	Yes
<b>26n</b>	289.37	5	2	83.01	44.73	0.98	4.15	Yes	Yes	No
<b>26o</b>	290.32	7	2	74.47	38.74	0.15	8.55	Yes	Yes	Yes
<b>26p</b>	290.32	7	2	74.47	38.74	0.15	8.55	Yes	Yes	Yes
<b>26q</b>	290.32	7	2	74.47	38.74	0.15	8.55	Yes	Yes	Yes
<b>26r</b>	482.21	4	2	96	35.5	2.41	3.81	Yes	Yes	No
<b>27a</b>	261.32	3	2	74.46	73.3	0.44	1.59	Yes	Yes	Yes
<b>27b</b>	280.75	3	1	75.06	47.28	1.53	1.93	Yes	Yes	Yes
<b>27c</b>	280.75	3	1	75.06	47.28	1.53	1.93	Yes	Yes	Yes
<b>27d</b>	280.75	3	1	75.06	47.28	1.53	1.93	Yes	Yes	Yes
<b>27e</b>	325.2	3	1	77.75	47.28	1.65	1.09	Yes	Yes	Yes
<b>27f</b>	325.2	3	1	77.75	47.28	1.65	1.09	Yes	Yes	Yes

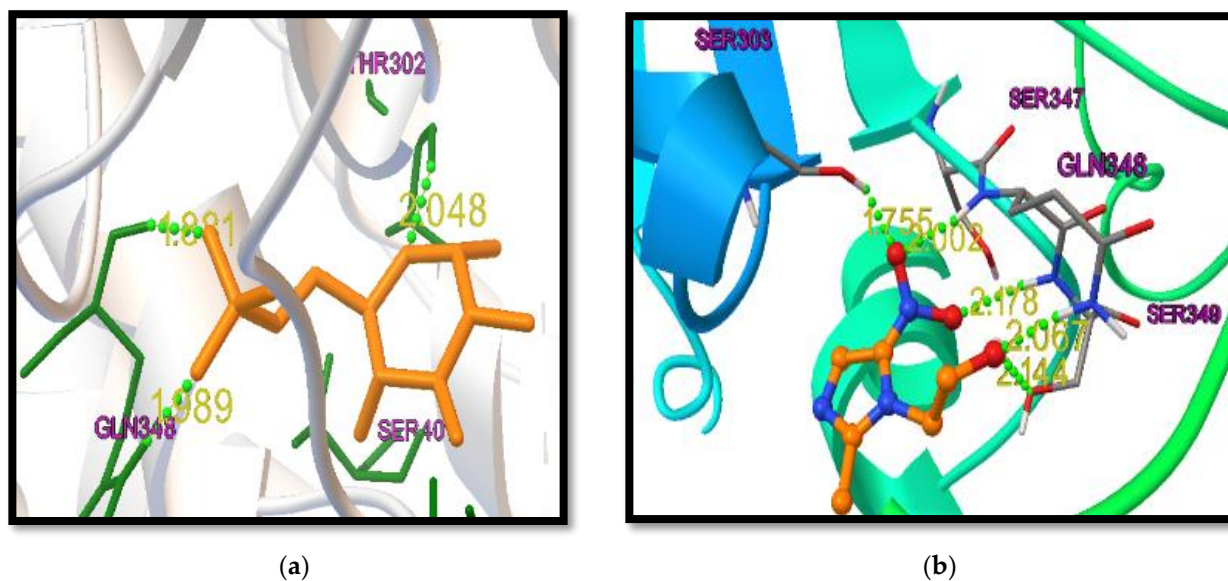
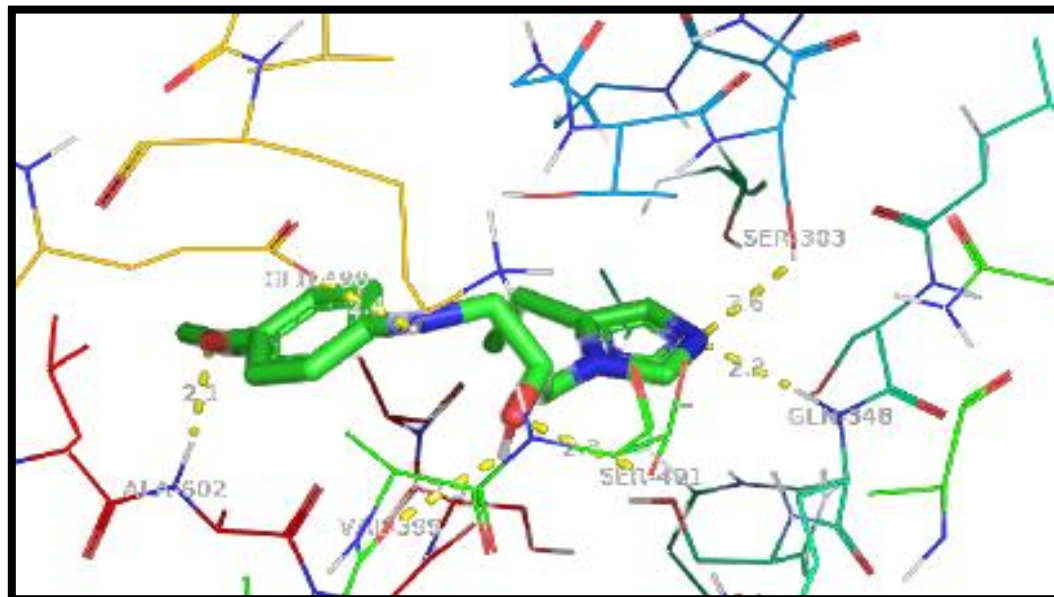
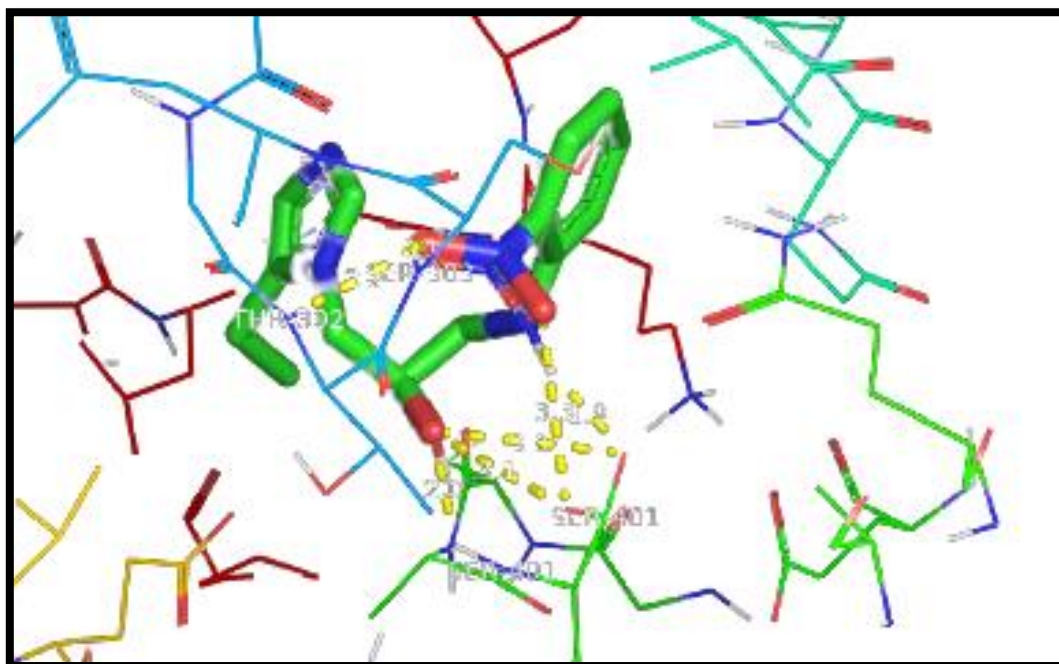


**Figure 1.** (a) Redocking of co-crystallized ligand GLP(28) in the binding pocket of Glucosamine-fructose-6-phosphate synthase (2VF5). Ligand is shown as orange line model and the amino acid residues interacting with the ligands are shown as green line model. Hydrogen bond interactions (2.048, 1.989, 1.881 Å) with amino acid residues of Glucosamine-fructose-6-phosphate synthase are shown in green dotted spheres. (b) Binding mode of standard drug Metronidazole (3) in the binding pocket of Glucosamine-fructose-6-phosphate synthase (2VF5). Ligand is shown as multicolour ball and stick model and the amino acid residues interacting with the ligands are shown as green line model. Hydrogen bond interactions (2.144, 2.067, 2.178, 2.002, 1.755 Å) with amino acid residues of Glucosamine-fructose-6-phosphate synthase are shown in green dotted spheres.

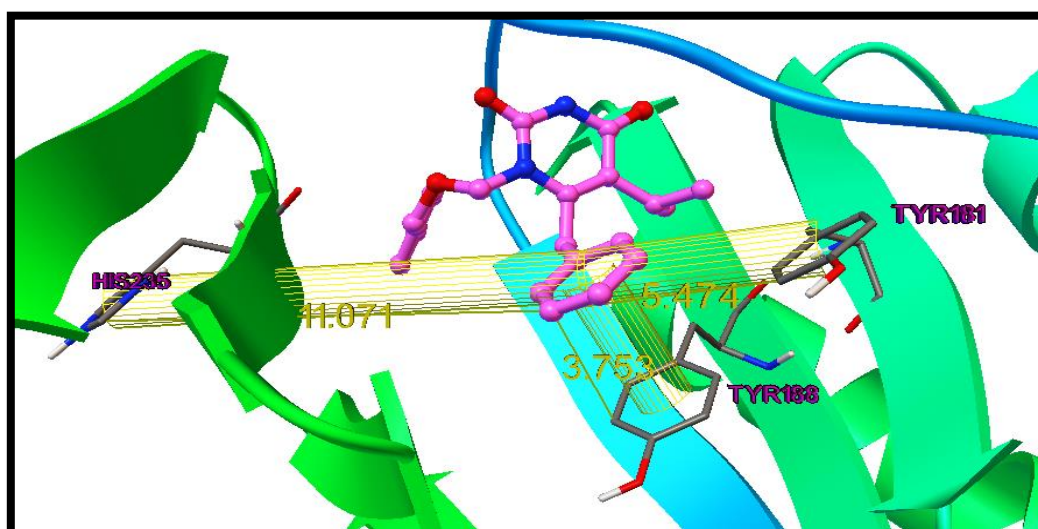


(a)

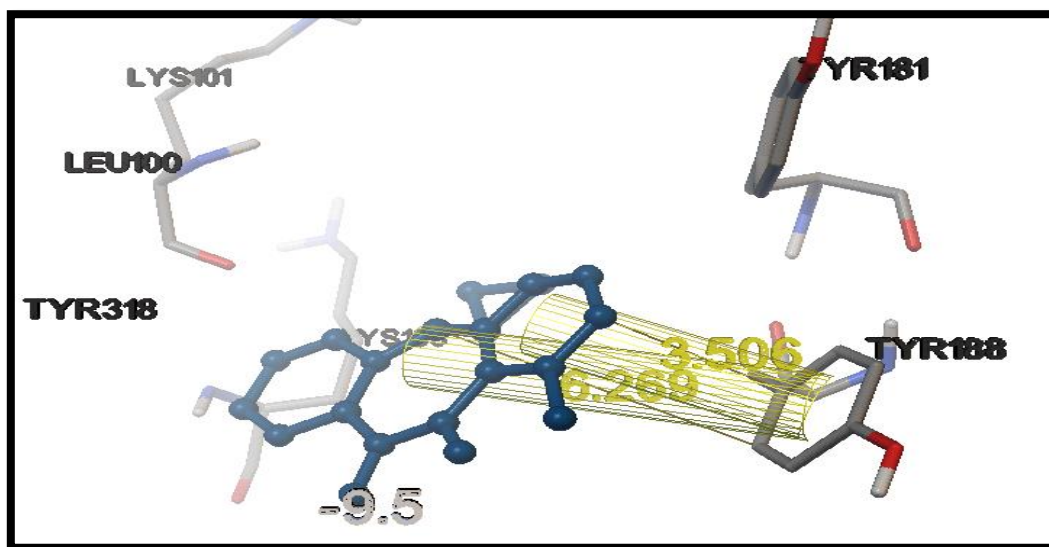


(b)

**Figure 2.** (a) Docking of compound **26n** in the binding pocket of Glucosamine-fructose-6-phosphate synthase (2VF5). Ligand is shown as green line model and the amino acid residues interacting with the ligands are shown as conventional colored line model. 6- Hydrogen bond interactions (2.4, 2.5, 2.6, 2.2, 2.1, 2.9 Å) with amino acid residues of Glucosamine-fructose-6-phosphate synthase are shown in yellow dotted lines. (b) Docking of compound **26o** in the binding pocket of Glucosamine-fructose-6-phosphate synthase (2VF5). Ligand is shown as green line model and the amino acid residues interacting with the ligands are shown as conventional colored line model. 8- Hydrogen bond interactions (2.0, 3.3, 3.1, 1.9, 3.3, 2.2, 2.1, 2.9 Å) with amino acid residues of Glucosamine-fructose-6-phosphate synthase are shown in yellow dotted lines.

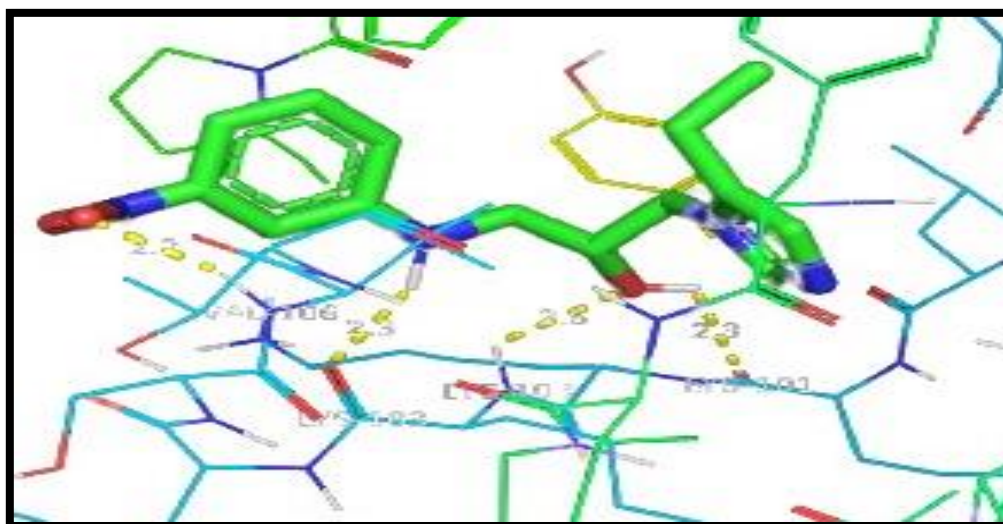


(a)

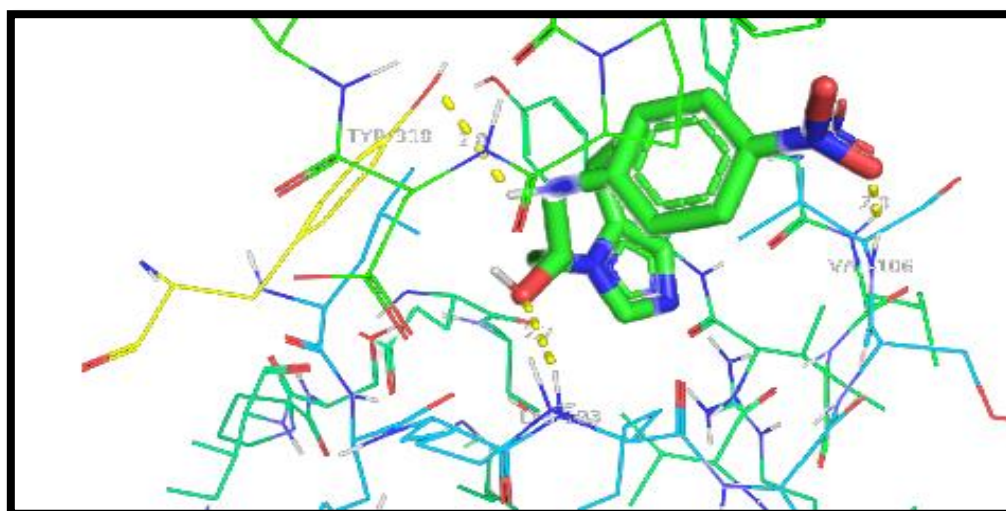


(b)

**Figure 3.** (a) Redocking of co-crystallized ligand TNK651 (29) in the binding pocket of HIV-1 Reverse Transcriptase (1RT2). Ligand is shown as pink line model and the amino acid residues interacting with the ligands are shown as conventional coloured line model.  $\pi$ -bond interactions (3.753, 5.474, 11.071 Å) with amino acid residues of HIV-1 Reverse Transcriptase are shown as lines. (b) Binding mode of standard drug Nevirapine (30) in the binding pocket of HIV-1 Reverse Transcriptase (1RT2). Ligand is shown as blue coloured ball and stick model and the amino acid residues interacting with the ligands are shown in conventional coloured line model.  $\pi$ -bond interactions (6.269, 3.506 Å) with amino acid residues of HIV-1 Reverse Transcriptase are shown as lines.



(a)



(b)

**Figure 4.** (a) Docking of compound **26p** in the binding pocket of HIV-1 Reverse Transcriptase (1RT2). Ligand is shown as green line model and the amino acid residues interacting with the ligands are shown as conventional colored line model. 4-Hydrogen bond interactions (2.2, 2.3, 2.6, 2.3 Å) with amino acid residues of HIV-1 Reverse Transcriptase are shown in yellow dotted lines. (a) Docking of compound **26q** in the binding pocket of HIV-1 Reverse Transcriptase (1RT2). Ligand is shown as green line model and the amino acid residues interacting with the ligands are shown as conventional colored line model. 3-Hydrogen bond interactions (2.0, 2.7, 2.8 Å) with amino acid residues of HIV-1 Reverse Transcriptase are shown in yellow dotted lines.

## 5. Conclusions

Imidazole analogs (**26a–r**) & (**27a–g**) were designed based on QSAR studies. Docking studies and predictive ADME studies were performed on the designed analogs. Binding mode analysis was carried out in the active site of glucosamine-fructose-6-phosphate synthase (PDB ID: 2VF5) and HIV-1 Reverse Transcriptase (PDB ID: 1RT2) for all the designed compounds. Binding mode studies suggested that, amongst the designed compounds, maximum compounds had shown comparable interactions to the interactions obtained from the standard drug used, few compounds had shown even better interactions than the standard drug used, in both the receptors. Compounds **26n** & **26o** had shown better interactions in the active site of glucosamine-fructose-6-phosphate synthase (PDB ID: 2VF5) and compounds **26p** & **26q** had shown better interactions in the active site of HIV-1 Reverse Transcriptase (PDB ID: 1RT2), than the standard drugs used in both of them, i.e., metronidazole (5) and nevirapine (30) respectively. The predictive ADME studies suggested that all the compounds were lead-like and can be synthesized for their further exploration.

**Acknowledgments:** The authors would like to Acknowledge, the Department of Pharmaceutical Sciences and Technology, Birla Institute Of Technology, Mesra, Ranchi.

**Conflicts of Interest:** The authors declare no conflict of interest.

## References

1. Black, J.H., Jr.; Beale, J.H. *Wilson and Gisvold's textbook of Organic Medicinal and Pharmaceutical Chemistry*; 2004; p. 504.
2. Butler, K.; Howes, H.L.; Lynch, J.E.; Pirie, D.K. Nitroimidazole Derivatives. Relationship between Structure and Antitrichomonal Activity. *J. Med. Chem.* **1967**, *10*, 891–897.
3. Tweit, R.C.; Muir, R.D.; Ziecina, S. Nitroimidazoles with Antibacterial Activity against *Neisseria Gonorrhoeae*. *J. Med. Chem.* **1977**, *20*, 1697–1700.
4. Butler, K.; Howes, H.L.; Lynch, J.E.; Pirie, D.K. Nitroimidazole Derivatives. Relationship between Structure and Antitrichomonal Activity. *J. Med. Chem.* **1967**, *10*, 891–897.
5. Mital, A. Synthetic Nitroimidazoles: Biological Activities and Mutagenicity Relationships. *Sci. Pharm.* **2009**, *77*, 497–520.

6. Edwards, D. Nitroimidazole drugs-action and resistance mechanisms: Mechanism of action. *J. Antimicrob. Chemother.* **1993**, *31*, 9–20.
7. Raether, W.; Hänel, H.; Ha, H. Nitroheterocyclic Drugs with Broad Spectrum Activity. *Parasitol. Res.* **2003**, *90* (Suppl. 1), S19–S39.
8. Hall, B.S.; Wilkinson, S.R. Activation of benznidazole by trypanosomal type I nitroreductases results in glyoxal formation. *Antimicrob. Agents Chemother.* **2012**, *56*, 115–123.
9. Finar, I.L. Stereochemistry and chemistry of natural products. *Org. Chem.* **2002**, *2*, 622–629.
10. Veraldi, S. Isoconazole nitrate: A unique broad-spectrum antimicrobial azole effective in the treatment of dermatomycoses, both as monotherapy and in combination with corticosteroids. *Mycoses* **2013**, *56*, 3–15.
11. Fischer, J.; Ganellin, C.R. *Analogue-Based Drug Discovery*; John Wiley & Sons: New York, NY, USA, 2006; p. 509, ISBN 9783527607495.
12. Seidman, L.S.; Skokos, C.K. An evaluation of Butoconazole nitrate 2% Site Release<sup>®</sup> vaginal cream (Gynazole-1<sup>®</sup>) compared to fluconazole 150 mg tablets (Diflucan<sup>®</sup>) in the time to relief of symptoms in patients with vulvovaginal candidiasis. *Infect. Dis. Obstet. Gynecol.* **2005**, *13*, 197–206.
13. Wigger-Alberti, W.; Kluge, K.; Elsner, P. Clinical effectiveness and tolerance of climbazole containing dandruff shampoo in patients with seborrheic scalp eczema. *Praxis* **2001**, *90*, 346–349.
14. Becker, K.L. *Principle and Practice of Endocrinology and Metabolism, Lippincotts Williams and Wilkins*; 2001; p. 1197, ISBN 9780781717502.
15. Croxtall, J.D.; Plosker, G.L. Sertaconazole. *Drugs* **2009**, *69*, 339–359.
16. Alomar, A.; Videla, S.; Delgadillo, J.; Gich, I.; Izquierdo, I.; Forn, J.; Muntañola, A.A.; Masoliver, A.A.; Corominas, A.B.; Montesinos, E.B.; et al. Flutrimazole 1% dermal cream in the treatment of dermatomycoses: A multicentre, double-blind, randomized, comparative clinical trial with bifonazole 1% cream. *Dermatology* **1995**, *190*, 295–300.
17. Rovati, R.A.; Mestres, R.C. Dichloro-Substituted Imidazole Derivatives as Antifungal Agents. U.S. Patent 07887103, 1993.
18. Hiroyoshi, K.; Yoshiki, N.; Masanori, Y. Antifungal Agent, Its Compound, Production Thereof and Its Usage. Japan Patent 1997100279, 1997.
19. Turner, B.G.; Summers, M.F. Structural biology of HIV. *J. Mol. Biol.* **1999**, *285*, 1–32.
20. Singh, R.; Gupta, S.; Singh, J.; Arsi, T. Azoles as non-nucleoside reverse transcriptase inhibitors (NNRTIs): Mini review. *Int. J. Pharm. Sci. Res.* **2017**, *8*, 29.
21. De Clercq, E. New approaches toward anti-HIV chemotherapy. *J. Med. Chem.* **2005**, *48*, 1297–1313.
22. De Clercq, E. The design of drugs for HIV and HCV. *Nat. Rev. Drug Discov.* **2007**, *6*, 1001–1018.
23. Miller, M.W.; Howes, H.L.; Kasubick, R.V.; English, A.R. Alkylation of 2-methyl-5- nitroimidazole. Some potent antiprotozoal agents. *J. Med. Chem.* **1970**, *13*, 849–852.
24. Mouilleron, S.; Badet-Denisot, M.A.; Golinelli-Pimponeau, B. Ordering of C-terminal loop and glutaminase domains of glucosamine-6-phosphate synthase promotes sugar ring opening and formation of the ammonia channel. *J. Mol. Biol.* **2008**, *377*, 1174–1185.
25. Lindstrom, W.; Morris, G.M.; Weber, C.; Huey, R. *AutoDock 4. The Scripps Research Institute; Molecular Graphics Laboratory*: CA, USA, 2008.
26. Hopkins, A.L.; Ren, J.; Esnouf, R.M.; Willcox, B.E.; Jones, E.Y.; Ross, C.; Miyasaka, T.; Walker, R.T.; Tanaka, H.; Stammers, D.K.; et al. Complexes of HIV-1 reverse transcriptase with inhibitors of the HEPT series reveal conformational changes relevant to the design of potent non-nucleoside inhibitors. *J. Med. Chem.* **1996**, *39*, 1589–600.
27. RCSB PDB. Available online: <http://www.rcsb.org/pdb> (accessed on 10 February 2021).
28. ProdrG 2 Server. Available online: <http://prodrG1.dyndns.org/> (accessed on 15 April 2021).
29. Available online: <http://www.swissadme.ch> (accessed on 20 March 2020).